

Conductance Studies on Trichotoxin_A50E and Implications for Channel Structure

H. Duclohier,* G. M. Alder,[†] C. L. Bashford,[†] H. Brückner,[‡] J. K. Chugh,[¶] and B. A. Wallace[¶]

*Interactions Cellulaires et Moléculaires, UMR 6026 Centre National de la Recherche Scientifique-Université de Rennes I, 35042 Rennes Cedex, France; [†]Department of Biochemistry and Immunology, St. George's Hospital Medical School, Cranmer Terrace, London SW 17 0RE, United Kingdom; [‡]Dept. of Food Sciences, Interdisciplinary Research Center, University of Giessen, 35392 Giessen, Germany; and [¶]Department of Crystallography, Birkbeck College, University of London, London WC1E 7HX, United Kingdom

ABSTRACT Trichotoxin_A50E is an 18-residue peptaibol whose crystal structure has recently been determined. In this study, the conductance properties of trichotoxin_A50E have been investigated in neutral planar lipid bilayers. The macroscopic current-voltage curves disclose a moderate voltage-sensitivity and the concentration-dependence suggests the channels are primarily hexameric. Under ion gradients, shifts of the reversal potential indicate that cations are preferentially transported. Trichotoxin displays only one single-channel conductance state in a given experiment, but an ensemble of experiments reveals a distribution of conductance levels. This contrasts with the related peptaibol alamethicin, which produces multiple channel levels in a single experiment, indicative of recruitment of additional monomers into different multimeric-sized channels. Based on these conductance measurements and on the recently available crystal structure of trichotoxin_A50E, which is a shorter and straighter helix than alamethicin, a tightly-packed hexameric model structure has been constructed for the trichotoxin channel. It has molecular dimensions and surface electrostatic potential compatible with the observed conductance properties of the most probable and longer-lived channel.

INTRODUCTION

Peptaibols are fungal peptides which contain a high proportion of the nonstandard amino acid Aib (α -aminoisobutyric acid or α -methylalanine); they constitute a large family ranging in length from 5–20 residues (Rebuffat et al., 1999; Whitmore et al., 2003; Whitmore and Wallace, 2004). Many of the longer members of the family including alamethicin, the most widely-studied peptaibol, are capable of forming ion channels, a property which underlies their antimicrobial activity (Woolley and Wallace, 1992; Duclohier and Wróblewski, 2001). As a result of the large number of closely-related naturally-occurring “mutants” with different activity profiles that exist, the peptaibols are useful for studying structure/function relationships in ion channels (Wallace, 2000). The structures they adopt either in solution or in the solid-state are mainly helical but with varying proportions of α -helical and 3_{10} -helical motifs, and different degrees of bending in the middle, which result in significant variations in the orientation of their electric dipole moments.

Trichotoxins are 18 residues long and belong to subfamily (SF) 1, the “long” peptaibols (see Chugh and Wallace, 2001; and <http://www.cryst.bbk.ac.uk/peptaibols/>). They have been isolated from the fungus *Trichoderma viride* strain NRRL 5242 (Brückner et al., 1979; Jung et al., 1979; Przybylski et al.,

1984; Jaworski and Brückner, 1999). The crystal structure of trichotoxin_A50E has recently been determined at a resolution of 0.9 Å (Chugh et al., 2002). Its amino acid sequence is



where *U* is Aib, the polar glutamine residues indicated in bold, and proline in italics. The C-terminal is the amino-alcohol L-valinol and the N-terminus is acetylated (Ac).

Despite the presence of nine 3_{10} -helix-promoting Aib residues, trichotoxin is the first solved structure of a peptaibol that is completely α -helical. It has a very small central bend of 8–10° located between residues 10–13, making it a nearly straight molecule. Gln residues in positions 6 and 17 delineate a polar face, and are proposed to form the ion channel lumen stabilized by intermolecular hydrogen bonds. Another difference between trichotoxin and the amphipathic helical structures of two other members of SF1 whose structures have been determined—alamethicin_F30, crystal structure (Fox and Richards, 1982), and chrysospermin_C, NMR structure (Anders et al., 2000)—is the central bend, which ranges from 22–33° in different alamethicin monomers and is ~40° in chrysospermin_C. The two 16-residue members of SF2 and SF3, respectively, whose crystal structures have been solved, Leu¹-zervamicin (Karle et al., 1991) and antiamoebin_I (Snook et al., 1998) have even greater bends due to the presence of three imino acid residues. In trichotoxin, only the side chains of the hydrophilic Gln residues contribute to the polar interior whereas in antiamoebin and zervamicin, the polar lumen is

Submitted January 23, 2004, and accepted for publication June 1, 2004.

Address reprint requests to H. Duclohier, E-mail: herve-duclohier@wanadoo.fr.

C. L. Bashford's present address is School of Medicine, Keele University, Staffordshire ST5 5BG, United Kingdom.

J. K. Chugh's present address is Centre for Molecular Informatics, University of Cambridge, Cambridge CB2 1EW, United Kingdom.

© 2004 by the Biophysical Society

0006-3495/04/09/1705/06 \$2.00

doi: 10.1529/biophysj.104.040659

produced by both hydrophilic side chains and by some of the polypeptide backbone carbonyl oxygens.

In view of these structural differences amongst family members, it is of interest to study channel-forming properties of trichotoxin_A50E in planar lipid bilayers under conditions comparable to those which produce the channels with alamethicin (Sansom, 1993; Duclouhier and Wróblewski, 2001) and use this information to distinguish between oligomeric models for the channel. In this article we demonstrate the channel-forming ability of trichotoxin and describe experiments aimed at elucidating its molecularity. We have also built a hexameric channel model based on the crystal structure of the trichotoxin monomer, which is consistent with the measured conductance properties.

MATERIALS AND METHODS

Materials and peptide characterization

Trichotoxin_A50E was prepared by solution-phase synthesis as previously described (Brückner, 1987), purified and characterized by liquid chromatography and mass spectrometry (see Fig. 1). The calculated molecular mass for trichotoxin_A50E is 1689.96. The nominal molecular mass (mono-isotopic) is 1688, whereas it is 1689 and 1711 for the proton and the sodium adducts, respectively. The accuracy of higher masses recorded in centroid mode is ~ 0.5 – 1.0 m/z. The sequence was established from fragmentation patterns of the *b*-series counting for amino-acid residues ($-H_2O$). Fragments not observed in the full electron spray ionization-mass spectrum scan were detected in MS/MS.

The lipids used for planar bilayers were 1-palmitoyl-oleoylphosphatidylcholine (POPC) and dioleoylphosphatidylethanolamine (DOPE), purchased from Avanti Polar Lipids (Alabaster, AL). Squalene, hexadecane and hexane (spectroscopic grade) were from Sigma-Aldrich (Munich, Germany).

Electrical measurements on planar lipid bilayers

The activity induced by trichotoxin was assayed in planar lipid bilayers. Briefly, in the macroscopic conductance configuration, the activity of hundreds or thousands of channels were recorded with current-voltage (I-V) curves displayed by virtually solvent-free bilayers doped with trichotoxin_A50E and submitted to slow voltage ramps (~ 2 mV/s). The bilayer was made by “folding” two lipid monolayers (Montal and Mueller, 1972), after

solvent evaporation, over a 50–150 μ m hole in a PTFE film sandwiched between two half glass cells. The hole had been previously pretreated with a few μ l of either 4% hexadecane or squalene in hexane. Unless otherwise noted, the electrolyte on both sides was 1 M KCl, 10 mM Hepes (pH adjusted to 7.4 with KOH). Voltage was delivered via an Ag/AgCl electrode on the *cis*-side (the side of peptide addition and the positive-side for electrical conventions) which also recorded voltage-clamp currents via a current-voltage converter and amplifier (Model PC-One from Dagan, Minneapolis, MN). The second Ag/AgCl electrode, on the *trans*-side, was connected to the common virtual ground.

For recording single-channel activity at a steady-state applied voltage, a lower peptide concentration was used. The lipids used to form bilayers were a neutral mixture (5–10 mg/ml in hexane) of POPC and DOPE, molar ratio 7:3. Transmembrane currents were recorded and analyzed with the “Strathclyde Electrophysiology Softwares” (Win WCP and EDR) kindly provided by Dr. J. Dempster (Strathclyde University, Glasgow, Scotland). All conductance measurements were made at room temperature (20–22°C).

Molecular modeling

A hexameric model for the channel was constructed using the high resolution crystal structure (Chugh et al., 2002) of the monomer (Protein Data Bank identification, 1M24, chain A), in a manner similar to that previously described to make an octameric model of the trichotoxin channel (Chugh et al., 2002). The dimensions of the channel lumen and the predicted single-channel conductance level were calculated using the program HOLE (Smart et al., 1996); the electrostatic surface potentials were determined using the program GRASP (Nicholls et al., 1991).

RESULTS

Macroscopic conductances

The first hint of a powerful membrane lytic activity exhibited by trichotoxin came from the observation that planar lipid bilayers exposed to peptide concentrations of the order of 1 μ M became very leaky before irreversible dielectric breakdown occurred, within one minute. The investigations then continued with reduced peptide concentrations for macroscopic conductance (~ 1 order of magnitude reduction) and single-channel experiments (~ 2 orders of magnitude reduction).

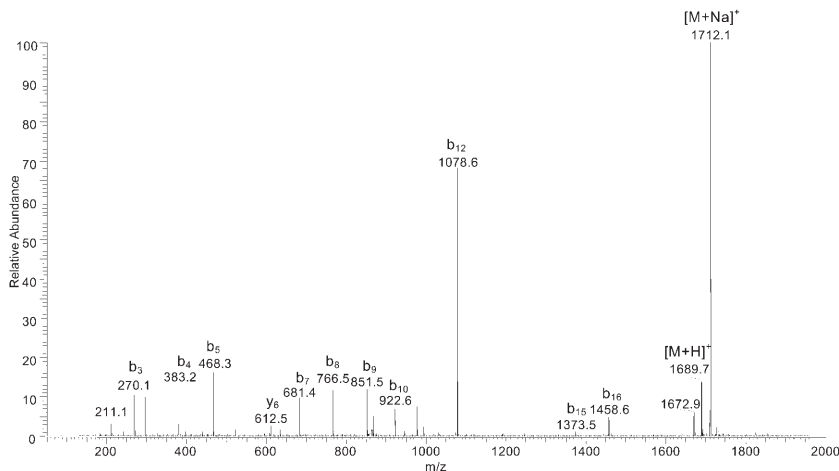


FIGURE 1 Electron spray ionization-mass spectrum of synthetic trichotoxin_A50E showing the protonated $[M+H]^+$ and sodiated $[M+Na]^+$ molecular ions at m/z 1689.7 and 1712.1, respectively, and an almost regular series of sequence specific acylium fragment ions b_3 – b_{17} as well as the y_6 fragment ion of the C-terminal hexapeptide at m/z 612.5 (for terminology, see Jaworski and Brückner, 1999). Experimental conditions: Finnigan LCQ instrument; heated capillary temperature 230°C; collision induced energy set at 45%; collision gas, helium; capillary voltage 3 V; spray voltage 4 kV; and direct infusion of 1% peptide in methanol/5% formic acid (1:1, v/v).

The apparent and mean number of peptaibol monomers per transmembrane conducting aggregate can be derived from both concentration- and voltage-dependences of macroscopic (i.e., “many-channels”) current-voltage (I-V) curves (Hall et al., 1984). Representative examples of such curves for three trichotoxin concentrations are shown in Fig. 2. Each of these I-V curves are averages of three successive runs to ensure partitioning of the peptide between the bath and the bilayer had reached equilibrium. The doped bilayers were submitted to voltage ramps slow enough (~ 2 mV/s) to ensure attainment of steady-state current values. Only the positive quadrant is shown since no significant current developed under applied negative voltages. Above a positive voltage threshold (defined as the intercept with an arbitrary reference conductance, dashed line) which is concentration-dependent, the macroscopic current developed exponentially. The practical concentration range over which the concentration-dependence, i.e., the shift of the voltage thresholds with peptide concentration, can be studied is limited both on the side of low concentration by the bilayer dielectric breakdown around 200 mV and on the side of high concentration by a clear definition of the intercept of the exponential current branch with the reference conductance. Here, with trichotoxin_A50E, that range is further reduced by the quite high concentration-dependence. Indeed, out of seven different experiments each with the three different concentrations, V_a the threshold shift for an e -fold concentration increase is 130 ± 10 mV.

The steepness of the exponential branches at the three studied concentrations remains quite modest especially when compared to alamethicin. In the instance presented in Fig. 2, V_e , the voltage increments resulting in an e -fold change in conductance ranged from 9–26 mV. As the analysis takes also into account the averaged concentration-dependence, it is justified to use for V_e the averaged value within the same concentration range. Out of seven different experiments summarized in Table 1, this value was 21 ± 3 mV. In the ‘barrel-stave’ model (Baumann and Mueller, 1974; Boheim, 1974) first put forward for alamethicin, a standard analysis

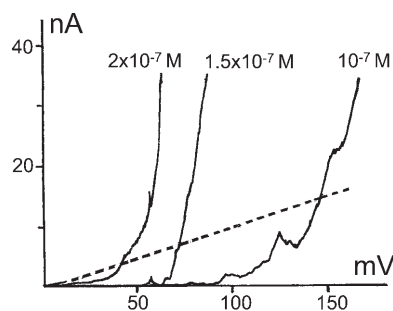


FIGURE 2 Macroscopic current-voltage (I-V) curves produced in neutral PC/PE (7:3) planar lipid bilayers bathed by symmetrical 1 M KCl and in the presence of indicated concentrations (*cis*-side) of trichotoxin_A50E. The peptaibol concentration range was limited both by the membrane dielectric breakdown (near 200 mV) and by a clear intercept with a reference conductance (dashed line, 100 nS).

TABLE 1 Concentration- and voltage-dependences of macroscopic current in seven independent experiments and averaged values

Experiment	V_a	V_e 1	V_e 2	V_e 3	V_e
1	130	26	9	19	18
2	133	22	12	16	17
3	128	27	13	26	22
4	135	20	12	16	16
5	126	30	19	23	24
6	138	29	20	26	25
7	124	30	12	27	23
Averages	130				21

V_a is the voltage shift of thresholds upon an e -fold change in trichotoxin concentration in the 10^{-7} M range. V_e 1, 2, and 3 are the voltage shifts producing e -folds in current at the following concentrations: 10^{-7} M, 1.5×10^{-7} M and 2×10^{-7} M, respectively. These are averaged for each experiment in the right-hand column, whereas the bottom row presents the overall averages from the seven experiments.

for voltage-dependent channel formation gives the apparent and mean number of peptide helical monomers per conducting bundle as $\langle N \rangle = V_a/V_e$ (Hall et al., 1984). Thus, here $\langle N \rangle = 130:21 = 6$ (rounded).

To investigate whether cations or anions were preferentially transported, at the end of some of the macroscopic conductance described above, trichotoxin-doped bilayers were submitted to a KCl gradient (100 mM *cis*-side/500 mM *trans*-side), the peptide remaining in the *cis*-side. V_{rev} , the reversal voltage or “zero-current voltage,” was noted after macroscopic conductance developed and reached steady-state. V_{rev} values were corrected for the liquid junction potentials without bilayers between both electrodes, both before and after the experiment. Out of three experiments, a reversal voltage at -27 ± 5 mV was noted. Experiments under the same conditions with alamethicin, known to be slightly cation-selective (Gordon and Haydon, 1975), yield a much smaller V_{rev} (-6 ± 1.5 mV). A simplified version of the Goldman-Hodgkin-Katz equation (Hille, 1992) allows derivation of a cation/anion permeability ratio $P_K/P_{Cl} \approx 6$ for trichotoxin, and 1.5 for alamethicin.

Single-channel conductances

Out of 22 attempted bilayer experiments performed in the same experimental conditions—same bilayers-forming lipids, POPC/DOPE (7:3), and all in symmetrical 1 M KCl—14 were successful, i.e., yielded single-channel events. Overall, three different conductance levels were observed. The most probable level had a large single-channel conductance of 850–900 pS (Fig. 3 A) and was observed in eight experiments. A medium-sized and fast flickering conductance of 400 pS with a substate at 200 pS was recorded during only two experiments (Fig. 3 A). Small but well-resolved events at 20 pS occurred in four out of 14 experiments (Fig. 3 B). There was no clear correlation with the peptide concentration

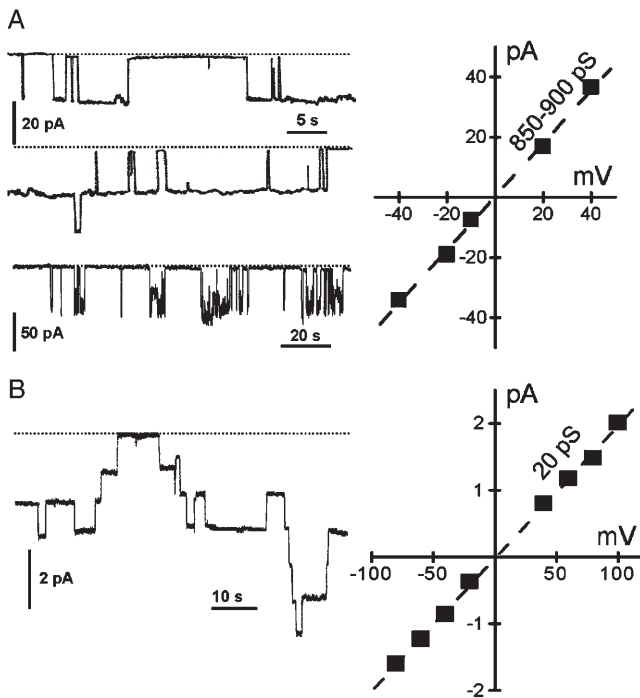


FIGURE 3 Single-channels induced by 10 nM Trichotoxin (*cis*-side) in PC/PE (7:3) planar lipid bilayers in symmetrical 1 M KCl. Panel A depicts large conductance channels whereas panel B highlights small conductance channels in different experiments. In all cases, openings are downward deflections. The two upper-most traces on the left of panel A represent a continuous recording of 100 s at an applied voltage of 20 mV. The single-channel current-voltage (I-V) plot on the right-hand side of panel A reveals a quite high conductance of 850–900 pS. At higher voltages, this evolves in “medium-sized” events as shown by the third trace of panel B: an applied voltage of 130 mV induces transitions rapidly flickering between 400 and 200 pS substates. In fewer experiments, a much smaller single-channel conductance is disclosed as shown in panel B. Here, up to six channels of 20 pS each are active in the bilayer.

within the range investigated nor with the time elapsed between peptide addition in the bath and time of recording. Contrasting with the well-known alamethicin pattern of activity, these levels were never observed simultaneously in the same bilayer. Note that this situation is reminiscent of the one previously encountered with magainins which constitute another class of antimicrobial or defense peptides albeit nonpeptaibol (Duclohier et al., 1989).

Hexameric model

In the absence of conductance data, an octameric model had been built for trichotoxin (Chugh et al., 2002), by analogy with the previous octameric models for alamethicin (Fox and Richards, 1982); and antiameobin (Wallace, 2000). However, since the conductance studies reported here are more consistent with a hexameric bundle, a new hexameric model was constructed from the monomer crystal structure in a manner similar to that previously described for the octameric model (Fig. 4, *upper row*). The lumen of the helical bundle model is

lined by Gln-6 and Gln-17 side chains from each of the monomers, forming intermolecularly hydrogen-bonded rings, and producing constrictions near the top and bottom of the pore (Fig. 4, *lower row*). The lumen has a strongly negative electrostatic surface potential (Fig. 4, *lower row, left*), consistent with a highly cation-selective channel. Significant differences between the hexamer and octamer include the minimum lumen dimensions (1.61 vs. 1.84 Å radius) (Fig. 4, *lower row, right*) and the orientations of the Gln side chains that line the lumen. The predicted single-channel conductance levels of the hexamer and octamer are 940 and 1300 pS, respectively. Hence the hexamer model is more consistent with the measured value of 850–900 pS, another indication that the channels are most likely hexameric.

DISCUSSION

Matha et al. (1992) hypothesized that membrane lysis and cell death induced by trichotoxin_A50E could be due to the formation of transmembrane channels or pores, which is consistent with the observations of channel formation in this study.

It is first useful to compare the conductance properties of trichotoxin_A50E with those of the well-known peptaibol alamethicin to which extensive studies have been devoted. At the macroscopic conductance level of investigation, the formation of trichotoxin_A50E channels appears significantly less voltage-dependent than for alamethicin. Indeed V_e , the voltage increment resulting in an e -fold change in conductance, is 21 mV for trichotoxin_A50E whereas it is 5–6 mV for alamethicin (Eisenberg et al., 1973; Béven et al., 1999). Presumably in trichotoxin the much-reduced helical kink favors at rest (no voltage applied) an orientation parallel to the bilayer surface. Thus, the voltage drop that occurs within the bilayer dielectric would be much less efficient than with alamethicin, whose N-terminus is partly embedded in the bilayer due to the Pro14-induced bend. We propose that this could be a likely, although not exclusive, cause for the differential voltage-sensitivity between the two peptaibols. Note that none of them bears formal electrical charges in their amino acid sequences. The oligomerization state of the trichotoxin channel is also smaller than for alamethicin: $\langle N \rangle = 6$ vs. 8–10 (Hall et al., 1984; Béven et al., 1999) and this is consistent with the smaller single-channel conductance of the most probable level displayed by trichotoxin: 850–900 pS vs. 2.8 pS in 1 M KCl (Sansom, 1993).

At the single-channel level of investigation, particularly noteworthy and contrasting again with alamethicin is the lack of nonintegral multilevels indicating that the uptake and release of monomers within the conducting bundle (and its ensuing fluctuating size) does not occur with trichotoxin. This is likely the result of trichotoxin having two sets of stabilizing interhelical hydrogen bonds involving Gln side chains, one near each end of the molecule. Because the trichotoxin helix is relatively straight (kink angle only 8–10°), both of the Gln residues can form stereochemically-acceptable hydrogen

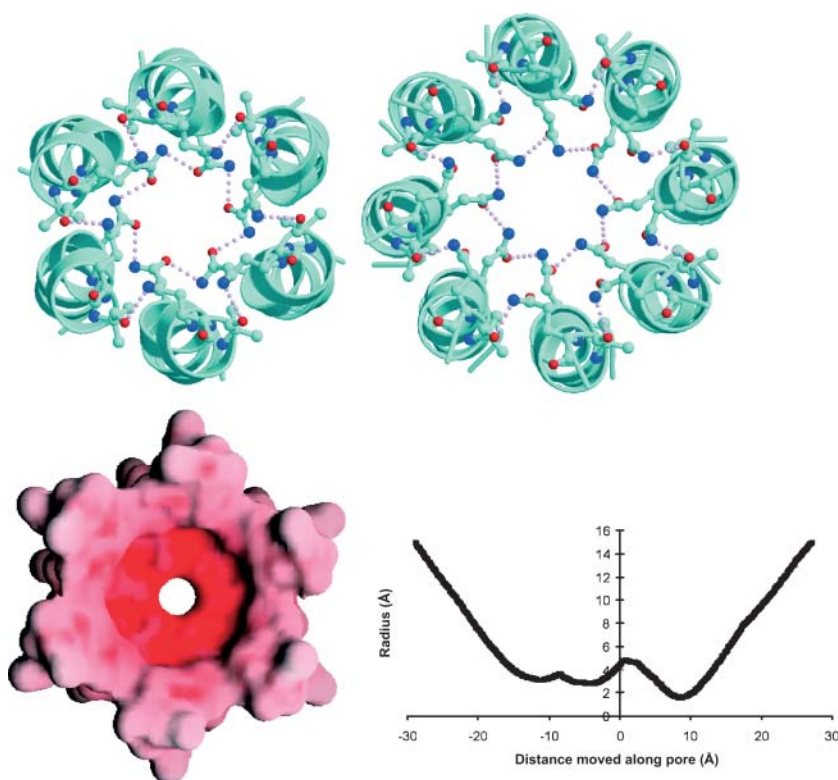


FIGURE 4 Helical bundle structures for the trichotoxin channel. (*Upper left*) Hexameric model viewed from the top. (*Upper right*) Octameric model viewed from the top. (*Lower left*) Top view of the hexamer showing the electrostatic surface potential. (*Lower right*) Plot of pore radius versus location along the pore for the hexamer. Figures in the upper row were created using the programs MolScript (Esnouf, 1997) and Raster3D (Merrit and Bacon, 1997).

bonds in the hexamer. Alamethicin, on the other hand, has a significant central bend ($22\text{--}33^\circ$) which may be facilitated by the presence of a glycine residue (absent in trichotoxin) preceding Pro-14 since it was previously shown in alamethicin derivatives, that both Gly-11 and Pro-14 had to be substituted (with Ala) to significantly straighten the helix (Jacob et al., 1999). The bend in the middle of the alamethicin molecule results in the C-termini of the monomers in its oligomeric channel being at a further distance from each other due to the funnel shape. As a result, its geometry is not as suitable for formation of the hydrogen bonds involving the penultimate Gln amino acid. This may mean the interhelical interactions are more flexible, leading to a range of oligomeric channels. For trichotoxin, and as was reported previously for magainins (Duclohier et al., 1989), a conductance levels distribution is only found from an ensemble of experiments. Thus, the trichotoxin single-channel behavior reflects a nearly stochastic recruitment of helical monomers. The trichotoxin monomers are presumably lying flat on the bilayer when no voltage is applied, whereas in the case of alamethicin the partial embedding of the N-terminus due to the Pro-14-induced bend would favor the dynamic uptake and release of monomers within the transmembrane barrel-stave (see e.g. for review Sansom, 1993; Duclohier and Wróblewski, 2001).

The preferential cation transport found here for trichotoxin_A50E is relatively high when compared to that for alamethicin, and may be related, in part, to the differences in dipole moment that are reflected in the electrostatic surface potentials of the molecular model (Fig. 4). The low

potassium selectivity over chloride ions of alamethicin detected in this study is consistent with an earlier study at the single-channel level of analysis (Boheim, 1974). In that study, the conductances of all the sublevels were $\sim 1.4\text{--}1.5$ times smaller when the impermeant cation tetramethylammonium replaced sodium (or potassium) in the chloride salt.

Analyses of macroscopic I-V curves indicated a hexameric transmembrane bundle as the most probable conducting structure. This has led to the construction of the hexameric model as shown in Fig. 4. The model is compatible with the measured unitary conductance of the most probable and longer-lived channel.

In summary, the lower single-channel conductance, the lack of multiple open states within a single recording, and, possibly, the lower voltage-dependence of trichotoxin is consistent with observations (Chugh et al., 2002) that trichotoxin forms straighter helices than does alamethicin, resulting in a helical bundle lumen that is relatively uniform and unlike the proposed funnel shape of alamethicin barrel-staves. The observed conductance properties of trichotoxin can be accounted for by the hexameric helical bundle structure modeled on the crystal structure of the trichotoxin monomer, and its functional differences with respect to other peptaibols can be rationalized on the basis of this structure.

H.D. thanks Dr. Y. Korchev (Imperial College, London, UK) for help at the revision stage. This work was supported, in part, by Wellcome Trust International Cooperation Grant 067956 (to B.A.W. and H.D.) and by the Cell Surface Research Fund (St. George's Hospital Medical School). J.K.C.

was the recipient of a Biotechnology and Biological Sciences Research Council studentship.

REFERENCES

- Anders, R., O. Ohlenschlager, V. Soskic, H. Wenschuh, B. Heise, and L. R. Brown. 2000. The NMR solution structure of the ion channel peptide chrysorespermin C bound to dodecylphosphocholine micelles. *Eur. J. Biochem.* 267:1784–1794.
- Baumann, G., and P. Mueller. 1974. A molecular model of membrane excitability. *J. Supramol. Struct.* 2:538–557.
- Béven, L., O. Helluin, G. Molle, H. Duclohier, and H. Wróblewski. 1999. Correlation between antibacterial activity and pore-sizes of two classes of voltage-dependent channel-forming peptides. *Biochim. Biophys. Acta.* 1421:53–63.
- Boheim, G. 1974. Statistical analysis of alamethicin channels in black lipid membranes. *J. Membr. Biol.* 19:277–303.
- Brückner, H. 1987. Chemical synthesis of trichotoxin, a membrane active polypeptide mycotoxin. In *Peptides*, Proc. 19th Eur. Pept. Symp. D. Theodoropoulos, editor. De Gruyter, Berlin. 231–234.
- Brückner, H., W. A. König, M. Greiner, and G. Jung. 1979. The sequences of the membrane-modifying peptide antibiotic trichotoxin_A40. *Angew. Chem. Int. Ed. Engl.* 18:476–477.
- Chugh, J. K., H. Brückner, and B. A. Wallace. 2002. Model for a helical bundle channel based on the high resolution crystal structure of trichotoxin_A50E. *Biochemistry.* 41:12934–12941.
- Chugh, J. K., and B. A. Wallace. 2001. Peptaibols: models for ion channels. *Biochem. Soc. Trans.* 29:565–570.
- Duclohier, H., G. Molle, and G. Spach. 1989. Antimicrobial peptide magainin I from *Xenopus* skin forms anion-permeable channels in planar lipid bilayers. *Biophys. J.* 56:1017–1027.
- Duclohier, H., and H. Wróblewski. 2001. Voltage-dependent pore formation and antimicrobial activity by alamethicin and analogues. *J. Membr. Biol.* 184:1–12.
- Eisenberg, M., J. E. Hall, and C. A. Mead. 1973. The nature of the voltage-dependent conductance induced by alamethicin in black lipid membranes. *J. Membr. Biol.* 14:143–176.
- Esnouf, R. 1997. An extensively modified version of MOLSCRIPT that includes greatly enhanced colouring capabilities. *J. Mol. Graph.* 15: 133–138.
- Fox, R. O., Jr., and F. M. Richards. 1982. A voltage-gated ion channel model inferred from the crystal structure of alamethicin at 1.5Å resolution. *Nature.* 25:325–330.
- Gordon, L. G. M., and D. A. Haydon. 1975. Potential-dependent conductances in lipid membranes containing alamethicin. *Phil. Trans. Roy. Soc. Lond. B.* 270:433–447.
- Hall, J. E., I. Vodyanoy, T. M. Balasubramanian, and G. R. Marshall. 1984. Alamethicin: a rich model for channel behavior. *Biophys. J.* 45:233–247.
- Hille, B. 1992. Selectivity permeability: independence. In *Ionic Channels of Excitable Membranes*, 2nd ed. Sinauer Associates, Sunderland, MA. 337–361.
- Jacob, J., H. Duclohier, and D. S. Cafiso. 1999. The role of proline and glycine in determining the backbone flexibility of a channel-forming peptide. *Biophys. J.* 76:1367–1376.
- Jaworski, A., and H. Brückner. 1999. Detection of new sequences of peptaibol antibiotics trichotoxins A40 by on-line liquid chromatography-electrospray ionisation mass spectrometry. *J. Chromatogr.* 862:179–189.
- Jung, G., H. Brückner, R. Oekonomopulos, G. Boheim, E. Breitmaier, and W. A. König. 1979. Structural requirements for pore formation in alamethicin and analogs. In *Peptides, Structure and Biological Function*, Proc. 6th Amer. Pept. Symp. E. Gross and J. Meienhofer, editors. Pierce Chemical, Rockford, IL. 667–654.
- Karle, I. L., J. L. Flippen-Anderson, S. Agarwalla, and P. Balaram. 1991. Crystal structure of Leu¹-zervamicin, a membrane ion-channel peptide: Implications for gating mechanisms. *Proc. Natl. Acad. Sci. USA.* 88: 5307–5311.
- Matha, V., A. Jegorov, M. Kiess, and H. Bruckner. 1992. Morphological alterations accompanying the effect of peptaibiotics, α -aminoisobutyric acid-rich secondary metabolites of filamentous fungi, on *Culex pipiens* larvae. *Tissue Cell.* 24:559–564.
- Merrit, E. A., and D. J. Bacon. 1997. Raster3D—photo-realistic molecular graphics. *Meth. Enzym.* 277:505–524.
- Montal, M., and P. Mueller. 1972. Formation of bimolecular membranes from monolayers and study of their electrical properties. *Proc. Natl. Acad. Sci. USA.* 69:3561–3566.
- Nicholls, A., K. Sharp, and B. Honig. 1991. Protein folding and association—insights from the interfacial and thermodynamic properties of hydrocarbons. *Proteins Struct. Funct. Genet.* 11:281–296.
- Przybylski, M., I. Dietrich, I. Manz, and H. Brückner. 1984. Elucidation of structure microheterogeneity of the polypeptide antibiotics paracelsin and trichotoxin_A50 by fast atom bombardment mass spectrometry in combination with selective *in situ* hydrolysis. *Biomed. Mass Spec.* 11:569–582.
- Rebuffat, S., C. Goulard, B. Bodo, and M.-F. Roquebert. 1999. The peptaibol antibiotics from *Trichoderma* soil fungi: structural diversity and membrane properties. *Recent Res. Devel. Org. & Bioorg. Chem.* 3:65–91.
- Sansom, M. S. P. 1993. Structure and function of channel-forming peptaibols. *Q. Rev. Biophys.* 26:365–421.
- Smart, O. S., J. G. Neduveilil, X. Wang, B. A. Wallace, and M. S. P. Sansom. 1996. HOLE: a program for the analysis of the pore dimensions of ion channel structural models. *J. Mol. Graph.* 14:354–360.
- Snook, C. F., G. A. Woolley, V. Pattabhi, S. P. Wood, T. L. Blundell, and B. A. Wallace. 1998. The structure and function of antiameobin I, a proline-rich membrane active polypeptide. *Structure.* 6:783–792.
- Wallace, B. A. 2000. Common structural features in gramicidin and other ion channels. *Bioessays.* 22:227–234.
- Whitmore, L., J. K. Chugh, C. F. Snook, and B. A. Wallace. 2003. The peptaibol database—a sequence and structure resource. *J. Pept. Sci.* 9: 663–665.
- Whitmore, L., and B. A. Wallace. 2004. The peptaibol database: a database for sequences and structures of naturally occurring peptaibols. *Nucleic Acids Res.* 32:D593–D594.
- Woolley, G. A., and B. A. Wallace. 1992. Model ion channels: gramicidin and alamethicin. *J. Membr. Biol.* 129:109–136.